DOI: 10.13009/EUCASS2022-6153
9TH EUROPEAN CONFERENCE FOR AERONAUTICS AND SPACE SCIENCES (EUCASS)

# Integration of a mechano-probabilistic optimization module in the COLIBRI tool and application to a launcher model

*Antoine DUMAS*[⋆†], *Oussama BRAYDI*[⋆], *Chahrazed AMRANE*[⋆§] *and Yannick GUERIN*[⋆⋆]
[⋆] *Phimeca Engineering, 34 rue de sarlième 63800 Cournon d'Auvergne.*
[⋆⋆] *CNES, Direction des lanceurs, DLA/SDT/STM, 52 rue Jacques Hillairet, 75612 Paris Cedex.*
[§] *Université Clermont Auvergne, CNRS, SIGMA Clermont, Institut Pascal, 63000 Clermont-Ferrand, France*
dumas@phimeca.com · braydi@phimeca.com · amrane@phimeca.com · yannick.guerin@cnes.fr
[†]Corresponding author

## Abstract

This paper presents the application of a mechano-probabilistic optimization methodology to deal with uncertainties on the design of reusable space vehicle demonstrator. The methodology is integrated as a python module on the COLIBRI design tool of the CNES. The methodology is mainly composed with four functionalities, the screening analysis, the sensitivity analysis, the failure probability estimation and the optimization under uncertainty, for each functionality several methods are implemented and applied to the launcher model. And the work shows an innovative character in the field of launchers, through the application of methods proven in industrial fields strongly constrained by reliability aspects.

## 1. Introduction

In structure and mechanical construction, there exist a lot of sources of uncertainties such as the geometrical tolerances, the material properties and others [13]. These uncertainties affect the performance, the robustness and the reliability of the products. Some types of uncertainties can be eliminated, by improving the knowledge about the model, or by investing on more accurate fabrication machines and metrology tools. While other types can not be eliminated, and their presence is inherent on the production process, as explained in [5]. In other side, ignoring the presence of uncertainties leads to un-robust and/or unreliable products. One of the ways to limit their effects is through design under uncertainties, by taking them into consideration in the early phase of the mechanical and structure design.

In the framework of ensuring space vehicle structures design under uncertainties and as part of the search for mass gain in these structures, while ensuring their reliability, CNES called on Phimeca to develop a mechano-probabilistic optimization module integrated into their COLIBRI design tool. The ultimate objective of this study is to perform a reliability-based design optimization of a part of a launcher.

Indeed, a global methodology based on four complementary functionalities, to deal with uncertainties, are implemented and applied on the launcher model. These functionalities are detailed in the following sections and they are enumerated below:

- Screening analysis.
- Sensitivity analysis.
- The estimation of the failure probability.
- Optimization under uncertainty.

This work shows an innovative character in the field of launchers, through the application of methods proven in industrial fields strongly constrained by reliability aspects. And the results reveal how design under uncertainties could be applied even for such complex model.

The paper is structured as follows: section 2 presents an overview of the theory, section 3 presents the application's model and results and finally the conclusion and some perspectives are outlined in section 4

DOI: 10.13009/EUCASS2022-6153



## 2. Overview of the theory

Several steps are described in the uncertainty methodology, and each of them uses different probabilistic techniques. The methods used in the application are developed in this section. In all this section, it is assumed that a physical model and a probabilistic model is defined. Let $\mathcal{M}$ be the physical model, $\mathbf{X} = \left(X^1, \ldots, X^m\right)$ the random vector that follows the joint distribution $f_{\mathbf{X}}$ of dimension $m$ and $\mathbf{Y} = (Y^1, \ldots, Y^n)$ the output random vector of interest where $\mathbf{Y} = \mathcal{M}(\mathbf{X})$.

### 2.1 Morris screening method

When dealing with high dimensional inputs and a heavy CPU time codes, it is often needed to reduce the input dimension by selecting only the most relevant ones, meaning the most influential ones. Screening methods are devoted to such purpose. Among them, the Morris method is one on the most known, because it requires few simulations to get an accurate estimate of the influential factors [7, 18].

The principle is to perform several one-at-a-time design of experiments and only requires the bounds on the input variables. The method acts as follows :

1. The input space must be discretized in a $p$ levels grid of space $\delta$.
2. A starting point is randomly chosen in this grid $\mathbf{x}^{j=1}$.
3. A perturbation is applied to each component but one a time, a trajectory is then obtained containing $m + 1$ experiments, as shown in Figure 1.
4. The output values are computed from this trajectory.
5. Elementary effects $ee_i$ associated to each input are computed, then for one trajectory $m$ elementary effects are available.
$$ee_i^1 = \frac{\mathcal{M}(\mathbf{x}^1, x_i^1 + \delta) - \mathcal{M}(\mathbf{x}^1)}{\delta} \tag{1}$$
6. Steps 2 to 5 are iterated $r$ times, each time starting from a new point $\mathbf{x}^j$, $j = \{1, \ldots, r\}$. Hence the total number of evaluations is equal to $r \times (m + 1)$.

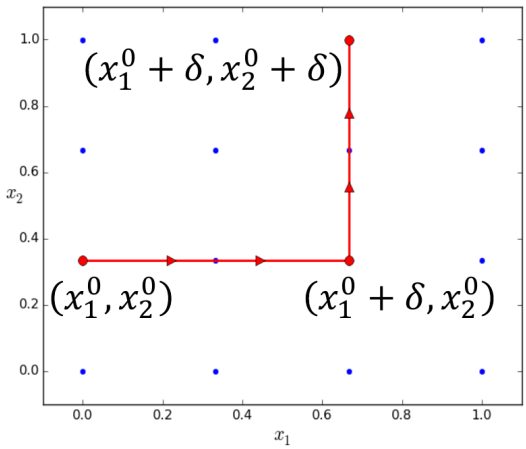


Figure 1: Example of a Morris trajectory in a 4-levels grid in dimension 2.

When the $r$ trajectories are evaluated, a sample of elementary effects of size $r$ and dimension $m$ is available. Statistics from this sample can be estimated for each input and according to their values, they can be used to determine the most influential variables and provide useful interpretation:

- **absolute mean** $\mu_i^*$ : high values highlights the important effects, so the output is sensitive to the corresponding input.
- **standard deviation** $\sigma_i$ : high values implies that it may exist interaction and/or non linearity effects. It is not possible to make the distinction between the two cases. In practice, interpretation is easier using the coefficient of variation $\delta_i = \sigma_i/\mu_i^*$. Roughly, if $\delta_i < 0.5$ the effect can be considered almost linear and without interaction.

DOI: 10.13009/EUCASS2022-6153



- **mean** $\mu_i$ : the mean of elementary effects can be used to determine the monotonic effects, indeed if $\mu_i = \pm\mu_i^*$, then the elementary effects have all the same signs which means that the output is only increasing or decreasing. Otherwise the case $|\mu_i| < \mu_i^*$ corresponds with a non monotonic effect.

In practice, dedicated graphics are used in order to help to interpret and visualize the effects. Two graphics are usually built, as it can be shown in the result section in the Figure 7 : $\sigma_i$ vs $\mu_i^*$ and $\mu_i$ vs $\mu_i^*$.

### 2.2 Global sensitivity analysis using Sobol' indices

A global sensitivity analysis allows to provide a quantitative ranking of the inputs regarding their influence on outputs. The well known Sobol' indices are dedicated to this end [23].

This method analyzes the influence of each component of an input random vector $\mathbf{X}$ on the output random vector $\mathbf{Y}$ by computing Sobol' indices. It computes, for every output random variable $Y^k (1 \leqslant k \leqslant n)$ the part of its variance due to each input component $X^i (1 \leqslant i \leqslant m)$ of $\mathbf{X}$.

Let consider only one output $Y$, using the Hoeffding decomposition, the variance can be written as follow :

$$\mathrm{Var}[Y] = \sum_{i}^{m} V_i + \sum_{1 \leq i < j \leq m} V_{i,j} + \ldots + V_{1,\ldots,m} \tag{2}$$

where $V_i = \mathrm{Var}_{X_i}[\mathbb{E}[Y|X_i]]$, $V_{i,j} = \mathrm{Var}_{X_i,X_j}\left[\mathbb{E}[Y|X_i, X_j]\right] - V_i - V_j$ and $V_{i,\ldots,m} = \mathrm{Var}_{X_i,\ldots,X_m}[\mathbb{E}[Y|X_i, \ldots, X_m]] - \sum_i^m V_i$.

The term $V_i$ corresponds to the part of the variance of the response explained by the only $X_i$ variable. And $V_{i,j}$ corresponds to the part of the variance of the response explained by the interaction between $X_i$ and $X_j$.

The first and second order Sobol' indices are then defined as :

$$S_i = \frac{V_i}{\mathrm{Var}[Y]} \tag{3}$$

$$S_{i,j} = \frac{V_{i,j}}{\mathrm{Var}[Y]} \tag{4}$$

The first order Sobol' index $S_i$ measures the part of the variance of $Y$ explained by $X_i$ alone. The second order Sobol' index $S_{i,j}$ measures the part of the variance of $Y$ explained by the interaction of $X_i$ and $X_j$. Indices varies from 0 to 1, the higher values the greater influence.

The sum of all Sobol' indices is equal to one:

$$\sum_{i}^{m} S_i + \sum_{1 \leq i < j \leq m} S_{i,j} + \ldots + S_{1,\ldots,m} = 1 \tag{5}$$

Instead of computing all order of Sobol' indices, total order indices $S_{Ti}$ are computed. Let define the following conditional variance :

$$V_{-i} = \mathrm{Var}\left[\mathbb{E}[Y|X_1, \ldots, X_{i-1}, X_{i+1}, \ldots X_{n_X}]\right] \tag{6}$$

Total order Sobol' indices are defined as follows:

$$S_{Ti} = 1 - \frac{V_{-i}}{\mathrm{Var}[Y]} \tag{7}$$

It corresponds with the sum of all indices related to a given variable $X_i$. For example, if $m = 3$, the total order for the variable $X_1$ is $S_{T1} = S_1 + S_{1,2} + S_{1,3} + S_{1,2,3}$

In practice, it is common to compute only the first and total order indices. A difference between both indices indicates that interaction exists between some inputs. Moreover the total interaction can be easily computed from the sum of all first order indices :

$$S_{interaction} = 1 - \sum_{i}^{m} S_i \tag{8}$$

**Estimation of the Sobol' indices**

Indices are generally estimated from a Monte Carlo simulation whose evaluation cost is $N \times (m + 2)$, where $N$ is the chosen simulation size. The size $N$ is usually at least several thousands in order to get an accurate estimate of the Sobol' indices. This techniques is hardly feasible if the model $\mathcal{M}$ is computationally expensive and / or if the number of input variables is large.

Another technique consists in using a surrogate model. One can build its favorite metamodel and use the Monte Carlo simulation to compute the Sobol' indices. However, the use of polynomial chaos expansion (PCE) can be preferred, because of its structure (functional decomposition in an orthogonal basis) allows to get the Sobol' indices from a post processing of the PCE coefficients.

DOI: 10.13009/EUCASS2022-6153



### 2.3 Methods for failure probability estimation

The mechanical system failure occurs when requirements of its good functioning and/or its safety are not gathered. The probability of occurrence of this failure event can be assessed by taking into account the various sources of the system uncertainties that are quantified and modeled by the input random vector $\mathbf{X}$. In that case, the outcome $\mathbf{Y} = \{Y_0, ..., Y_n\}$ is uncertain and the failure event is defined by:

$$\mathbf{Y} = \mathcal{M}(\mathbf{X}) \leq \mathbf{y}_t \tag{9}$$

where $\mathbf{y}_t = \{y_{t_1}, ..., y_{t_n}\}$ denotes here the thresholds that shouldn't be exceeded for the $n$ outputs.

In structural reliability analysis, it is very common to define a performance function, noted $g$, to define the system state. This function expresses the difference between the outcome $\mathbf{y}$ and the threshold $y_0$, i.e. $g = \mathbf{y} - \mathbf{y}_0$. If the performance function is unique, the reliability analysis is here called *component reliability analysis*. Otherwise, if more than one performance function are considered, the analysis is referred to *system reliability analysis*. The system might be one component that is subjected to multiple failure modes, or it might be composed of multiple components subjected to failure. Depending on the problem in hands, the interaction between the failure modes could be an intersection or a union.

In this section, the union system is to be considered. Thus, the system fails when the union of the individual failure modes is less or equal to zero, i.e. $\cup_{i=1}^{n} g_i(\mathbf{x}) \leq 0$, where $\mathbf{x} = (x_1, ..., x_m)$ denotes the vector of random input variables ang $g_i$ is the performance function of the i$^{th}$ failure mode, i.e. $g_i = y_i - y_{t_i}$. When $\cup_{i=1}^{n} g_i(\mathbf{x}) > 0$ means that the structure is safe for the input vector $\mathbf{x}$. The limit between the two situations, i.e. $\cup_{i=1}^{n} g_i(\mathbf{x}) = 0$, is called the Limit State Function (LSF). The failure probability is defined as the integral of the joint density function (PDF) $f_{\mathbf{X}}(\mathbf{x})$ over the failure domain $D_f = \{\mathbf{x} : \cup_{i=1}^{n} g_i(\mathbf{x}) \leq 0\}$:

$$P_f = \int_{D_f} f_{\mathbf{X}}(\mathbf{x}) d\mathbf{x} \tag{10}$$

Except for some simple academic cases, the calculation of this integral numerically based on traditional integration schemes or analytically is impossible. Indeed, the performance function is implicit since it is usually computed with computer codes and algorithms, e.g. finite element code. To approximate this integral, several methods have been proposed in the literature, see e.g. [8, 16, 17]. In this section, the methods used to estimate the failure probability are briefly recalled: Monte Carlo simulation, First Order Reliability Method (FORM), importance sampling method and subset simulation.

#### 2.3.1 Monte Carlo simulation

The Monte Carlo simulation method is a very popular method for the integral calculation. Its result is considered as the reference for the failure probability estimation, if the number of simulations is enough. The multidimensional integral of Equation 10 is computed here by generating first a large sample of realizations of the input random vector $\mathbf{X}$ according to its PDF $f_{\mathbf{X}}$. Then, the performance function is evaluated on this sample. By introducing the indicator function $\mathbb{I}_{D_f}$ of the failure domain $D_f$ (i.e. $\mathbb{I}_{D_f}(\mathbf{x}) = 0$ if $\mathbf{x} \in D_f$, $\mathbb{I}_{D_f}(\mathbf{x}) = 1$ otherwise), equation 10 becomes:

$$P_f = \int_{\mathbb{R}^n} \mathbb{I}_{D_f}(\mathbf{x}) f_{\mathbf{X}}(\mathbf{x}) d\mathbf{x} = \mathbb{E}_f[\mathbb{I}_{D_f}(\mathbf{X})] \tag{11}$$

where $\mathbb{E}[.]$ represents the mathematical expectation. For $N$ realizations of the input random vector $\mathbf{X}$, the Monte Carlo estimator of $P_f$ is expressed by:

$$\hat{P}_f^{MC} = \frac{1}{N} \sum_{i=1}^{N} \mathbb{I}_{D_f}\left(\mathbf{X}^{(i)}\right) = \frac{|N_f|}{N} \tag{12}$$

where $|N_f|$ indicates the cardinal of the set $N_f = \{i : g(x^{(i)}) \leq 0\}$. According to the law of large numbers, this estimator is unbiased, i.e. $E[\hat{P}_f^{MC}] = P_f$. Its coefficient of variation reads:

$$\delta_{\hat{P}_f^{MC}} = \frac{\sigma^2_{\hat{P}_f^{MC}}}{E[\hat{P}_f^{MC}]} = \sqrt{\frac{1 - P_f}{N P_f}} \tag{13}$$

According to the above equation, a precise estimator $\hat{P}_f^{MC}$requires a small coefficient of variation $\delta_{\hat{P}_f^{MC}}$. This is generally not an easy task when the performance function is costly to evaluate. Furthermore, the number of simulations increases drastically when small failure probabilities are to estimate. It should also be noted that the coefficient of variation $\delta_{\hat{P}_f^{MC}}$

DOI: 10.13009/EUCASS2022-6153



does not depend on the dimension of the input random vector, which makes the method insensitive to problems with high dimensions.

### 2.3.2 First order reliability method (FORM)

The estimation of the failure probability with this method is performed in the standard space, where the random variables are independent standard Gaussian and are gathered in the random vector $\mathbf{U} \sim \mathcal{N}(0,1)$. In that case, an isoprobabilistic transformation of the original space, called also physical space, to the standard space is performed. Various techniques are proposed in the literature to apply this transformation, see e.g. [19] for Nataf transformation and [21] for Rosenblatt transformation. This allows us to express the failure probability in the standard space as follows:

$$P_f = \int_{D_f^{'}} \varphi_{\mathbf{U}}(\mathbf{u}) d\mathbf{u} \tag{14}$$

where $D_f^{'} = \{\mathbf{u} : \cup_{i=1}^{n} G_i(\mathbf{u}) \leq 0\}$ and $G_i$ is the transformed performance function of the i$^{th}$ failure mode in the standard space.

The main idea of this method is to approximate the LSF locally with a linear Taylor expansion. The latter is performed on a specific point in the LSF, generally named design point or most probable failure point (MPFP) and corresponds to the maximum density of probability in the standard space [16]. This point is completely defined by its coordinates which are the solution of the following constrained optimization problem:

$$\mathbf{u}^* = \underset{\mathbf{u}\in\mathbb{R}}{\operatorname{argmin}}\, \mathbf{u}^T\mathbf{u} \quad \text{s.c.} \quad G(\mathbf{u}) = 0 \tag{15}$$

To solve this optimization problem, usual algorithms such as Rackwitz-Fiessler algorithm [20] or Abdo-Rackwitz algorithm could be used [1]. The distance between the MPFP $P^*$ and the origin of the standard space is noted $\beta$ and it is named the reliability index.

Once that the MPFPs $P_i^*$ are defined for each performance function $G_i$, its LSF is replaced with its tangent hyperplane at $P_i^*$, as illustrated in Figure 2. The equation of one hyperplane is given by:

$$\tilde{G}_i(\mathbf{u}) = \beta_i - \boldsymbol{\alpha}_i^T\mathbf{u} \tag{16}$$

where $\boldsymbol{\alpha}_i = -\nabla G_i(\mathbf{u}_i^*)/ \parallel \nabla G_i(\mathbf{u}_i^*) \parallel$ is the vector unit that verifies $\boldsymbol{\alpha}_i^T\boldsymbol{\alpha}_i = 1$ and $\nabla$ is the gradient operator. Failure probability is calculated in that case from that approximation and Equation 14 rewrites:

$$P_f = \int_{\cup_{i=0}^{n}\tilde{G}_i(\mathbf{U})\leq 0} \varphi_n(\mathbf{u}) d\mathbf{u} \tag{17}$$

The above integral can be calculated in a closed form and gives this approximation for the failure probability estimate [12]:

$$P_f^{FORM} = 1 - \Phi_m(\boldsymbol{\beta}; \boldsymbol{\rho}) \tag{18}$$

where $\boldsymbol{\beta} = \{\beta_1, ..., \beta_n\}$ and $\boldsymbol{\rho} = \{\rho_{ij}, i, j = 1, ..., n\}$ is the correlation matrix of LSFs, such that $\rho_{ij} = \alpha_i^T\alpha_j$. For a good understanding of these notions, one can refer to Figure 2, which exhibits an illustration in a two-dimensional space of the previous parameters $P^*, \beta, \boldsymbol{\alpha}$ and the tangent hyperplane for one performance function.

It should be noted that FORM assumes the uniqueness of the $P^*$ and the linearity of the LSF. If these assumptions are not satisfied, the failure probability estimate could be biased w.r.t its true value.

### 2.3.3 Importance sampling

To reduce the computational burden of Monte Carlo simulation in the context of small failure probabilities, the importance sampling method is proposed in [11, 22]. Its idea is to generate more simulations in the failure domain. This is performed with the introduction of an instrumental distribution, noted $h_{\mathbf{U}}$. The latter is used as follows in the formulation of the failure probability:

$$\begin{aligned} P_f &= \int_{\mathbb{R}^n} \mathbb{I}_{D_f}(\mathbf{u}) \frac{f_{\mathbf{U}}(\mathbf{u})}{h_{\mathbf{U}}(\mathbf{u})} h_{\mathbf{U}}(\mathbf{u}) d\mathbf{u} \\ &= E_h\left[\mathbb{I}_{D_f}(\mathbf{U}) \frac{f_{\mathbf{U}}(\mathbf{U})}{h_{\mathbf{U}}(\mathbf{U})}\right] \end{aligned} \tag{19}$$

DOI: 10.13009/EUCASS2022-6153



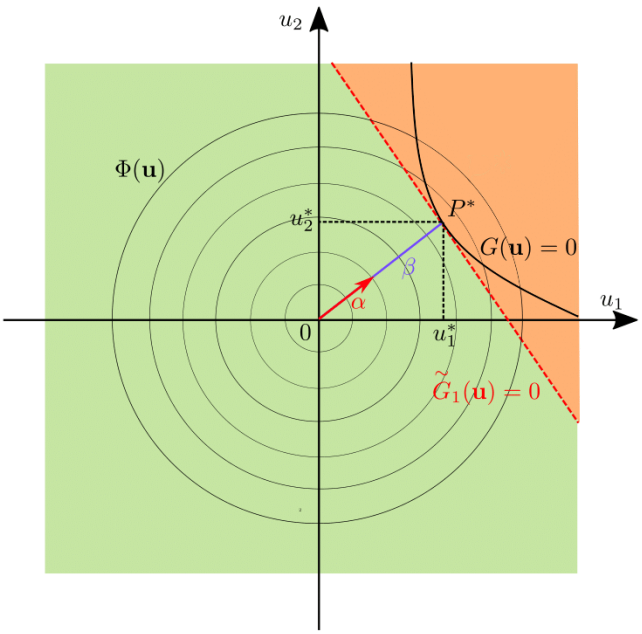


Figure 2: FORM method illustration on a 2D example. The orange region illustrates the failure domain.

For $N$ simulations drawn according to the instrumental density $h_{\mathbf{U}}$, the failure probability estimator can be expressed by:

$$\hat{P}_{fIS} = \frac{1}{N}\sum_{i=1}^{N} \mathbb{I}_{D_f}(\mathbf{U}^{(i)}) \frac{f_{\mathbf{U}}(\mathbf{U}^{(i)})}{h_{\mathbf{U}}(\mathbf{U}^{(i)})} \tag{20}$$

Using an instrumental density defined in the standard space is a common choice. The aim is to generate simulations in the vicinity of the MPFP $P^*$, previously introduced in section 2.3.2. Thus, the instrumental density is a multivariate standard normal PDF $\varphi_m$ centered on $P^*$ and it writes:

$$h_{\mathbf{U}} = \varphi_m(\mathbf{u} - \mathbf{u}^*) = \frac{1}{(2\pi)^{n/2}} \exp\left(-\frac{(\mathbf{u} - \mathbf{u}^*)^t(\mathbf{u} - \mathbf{u}^*)}{2}\right) \tag{21}$$

where $\mathbf{u}^*$ is the coordinate vector of $P^*$. The failure probability estimator, given in 20, rewrites:

$$\hat{P}_{fIS} = \frac{1}{N}\sum_{i=1}^{N} \mathbb{I}_{D_f}(\mathbf{U}^{(i)}) \frac{\varphi_m(\mathbf{U}^{(i)})}{\varphi_m(\mathbf{U}^{(i)} - \mathbf{u}^*)} \tag{22}$$

The convergence of this method is relatively better since the rate of failing simulations is almost 50%, see Figure 3. If more than one MPFP have to be considered, one can use a mixture of multivariate standard normal PDFs centered on the different MPFPs, see e.g. [3].

### 2.4 Optimization under uncertainties

The ultimate phase on the design under uncertainties is the model optimization under it. Deterministic optimization (DO) type is the classical type of optimization, its formulation is given in equation 23. where $X$ is the vector of control variables, having $\bar{X}$ as nominal values, $P^{(k)}$ is the vector of the environmental parameters with dimension $k$. the objective and constraint functions are given by $f(\bar{X}, P^{(k)})$ and $g(\bar{X}, P^{(k)})$ respectively. The optimal and admissible design configuration is obtained by $\bar{X}_{OptAdm}$.

$$\begin{aligned} &\text{Find } \bar{X}_{OptAdm} \text{ such that :} \\ &\bar{X}_{OptAdm} = \arg\max_{\bar{X}} f(\bar{X}, P^{(k)}) \\ &\text{Subject to : } g(\bar{X}, P^{(k)}) \geq 0 \end{aligned} \tag{23}$$

DOI: 10.13009/EUCASS2022-6153



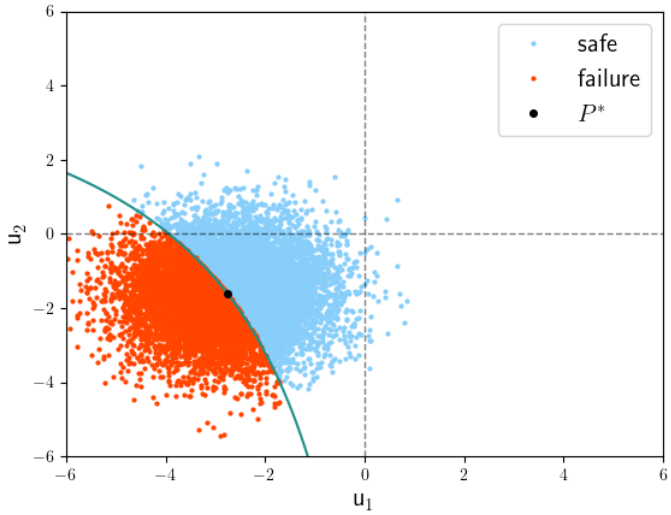


Figure 3: Illustration of the importance sampling method in the standard space.

As explained in [6], their exist three types of optimization under uncertainties:

- Robust design optimization design (RDO).
- Reliability based design optimization (RBDO).
- Reliability-based robust design optimization (RBRDO)

The main difference between these types is where the uncertainties is taken into consideration:

- In RDO: the uncertainties are mainly studied on the objective functions.
- In RBDO: the uncertainties are mainly studied on the constraint functions.
- In RBRDO: the uncertainties are mainly studied on both objective and constraint functions.

In this work, we are interested on RBDO type, which aims to found reliable and optimal design. It consists of optimizing deterministic objective function under probabilistic constraints. Many papers have studied RBDO like [2], [9], [14] and [24]. As given in [15], RBDO problem can be formulated by equation 24, where the associated uncertainties on $X$ and $P$ are given with the vector of random variables $w$. The probabilistic constraint functions are given by $g(X(\bar{X}, w), P(w))$. The allowed failure probability threshold is given by $Pf_{target}$ and the optimal and reliable design configuration is obtained by $\bar{X}_{OptRel}$. Alternative formulations for RBDO problem could be found in the literature, like in [6] and [25].

$$\begin{aligned} &\text{Find } \bar{X}_{OptRel} \text{ such that :} \\ &\bar{X}_{OptRel} = \arg\max_{\bar{X}} f(\bar{X}, P^{(k)}) \\ &\text{Subject to : Prob } g(X(\bar{X}, w), P(w)) \leq 0 \leq Pf_{target} \end{aligned} \tag{24}$$

The main difference between the results of deterministic optimization and RBDO is that the first one, leads to an optimal point which is located on the boundary of the deterministic feasible domain which is defined by: $[X \in \mathbb{R}^n \quad | \quad g(X, P) \geq 0]$. Such as optimal point produces unreliable design, where its failure probability is usually about 50%. At this optimal point, slightest uncertainty is enough to put the model on the failure domain. However the optimal point resulting from RBDO problem is far from the boundary of the deterministic feasible domain, and the corresponding distance is controlled by the admissible failure probability threshold. This difference between $\bar{X}_{OptRel}$ and $\bar{X}_{OptAdm}$ is shown in Figure 4 taken from [15], where an example of optimization problem is illustrated, the problem has two control variables ($R$ and $h$) and failure probability threshold ($Pf_{target} = 0.1$).

DOI: 10.13009/EUCASS2022-6153



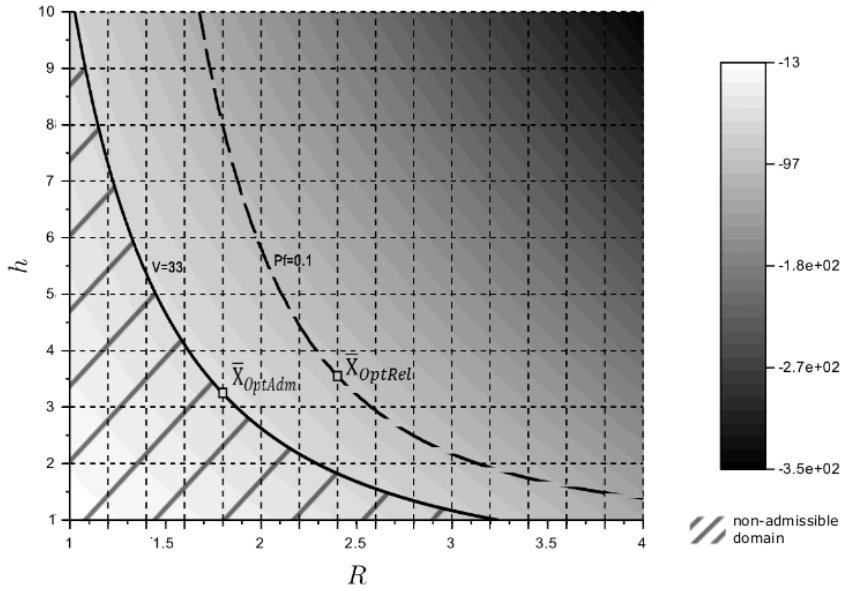


Figure 4: Example of difference between DO and RBDO results [15].

## 3. Application on the VEB

The uncertainty methodology is applied as part of the CALLISTO project, which is a reusable vehicle demonstrator in which CNES is the prime contractor in partnership with the DLR and the JAXA. An illustration of the vehicle is shown in Figure 5. The study focuses on the vehicle equipment bay (VEB) which is located on the top. The final objective is to reduce the mass of the VEB while ensuring its reliability.

Figure 5: Illustration of the CALLISTO project.

This section starts presenting the physical model and the probabilistic model of the inputs. Then a section shows results of the probabilistic analyses.

### 3.1 Presentation of the model

The VEB is modeled by a finite element model, using Nastran, where a static and a buckling analysis is performed. Some characteristics of this model are provided below:

DOI: 10.13009/EUCASS2022-6153



- Unit evaluation : about 5 minutes.
- Number of random variables : 47 divided into 3 categories :
  - 20 thickness variables,
  - 1 Young Modulus,
  - 26 loading variables : general forces, aerodynamic forces and QSL.

  Inputs are assumed to follow a Gaussian distribution with a coefficient of variation of 3% for the thicknesses and 5% for the other variables.
- Output of interest : 2 maximum Von Mises (VM) stress ($MAX\_Stress\_VM\_Z1$ and $MAX\_Stress\_VM\_Z2$), one maximum flux ($MAX\_IF\_Flux$).

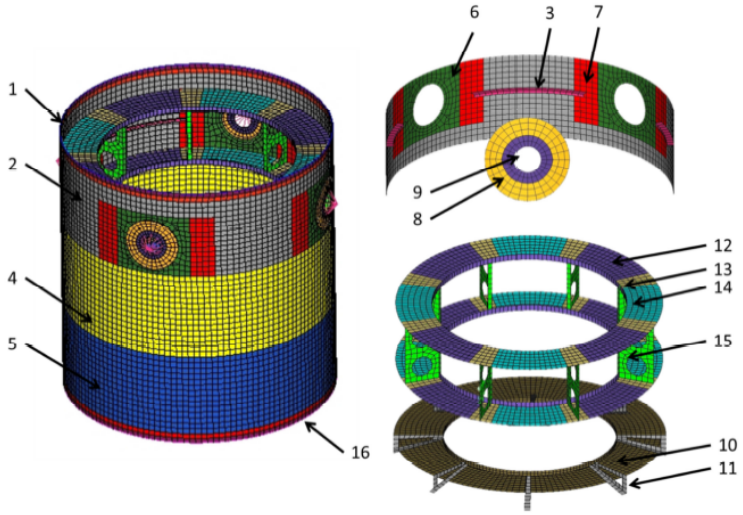


Figure 6: Finite element model of the vehicle equipment bay.

All the probabilistic analyses were performed using the OpenTURNS library [4]. These methodologies are currently integrated into the Colibri design tool of CNES.

### 3.2 Result

The uncertainty methodology has been applied in the following order :

1. Morris analysis : the goal is to reduce the number of inputs to take into account in the probabilistic analysis. Due the time required for a unit evaluation (parallel evaluations were not possible), it will be required to use a surrogate model. It is then easier to build the metamodel with the lowest possible number of inputs.
2. Sobol analysis : it will provide an accurate ranking of the inputs.
3. Probability of failure estimation : this allows to get a first probability of failure estimation before the optimization step and to adjust parameters method.
4. Optimization under uncertainty : this is the main goal which is optimizing the mass subjected to the respect of probability of failure.

#### 3.2.1 Screening analysis

The Morris analysis has been performed with the following parameters:

- grid discretization number : 6
- number of trajectories $r = 15$

DOI: 10.13009/EUCASS2022-6153



- total number of model evaluations : 720

Among the 47 random inputs, only 7 appears (4 thicknesses and 3 forces) to be influential on the 3 outputs (all taken together). The Figure 7 shows the Morris result for one output, only the 7 selected inputs are represented. It can easily be seen that 3 inputs are mainly influential ($\mu^*$ is high, they are on the right side of each figure). The 4 other influential inputs are close to the defined threshold that splits the influential and non influential area. Moreover, based on the figure, it is possible to conclude that the inputs have a monotonous effect but as $\sigma$ is high it may exist non linearity or interaction.

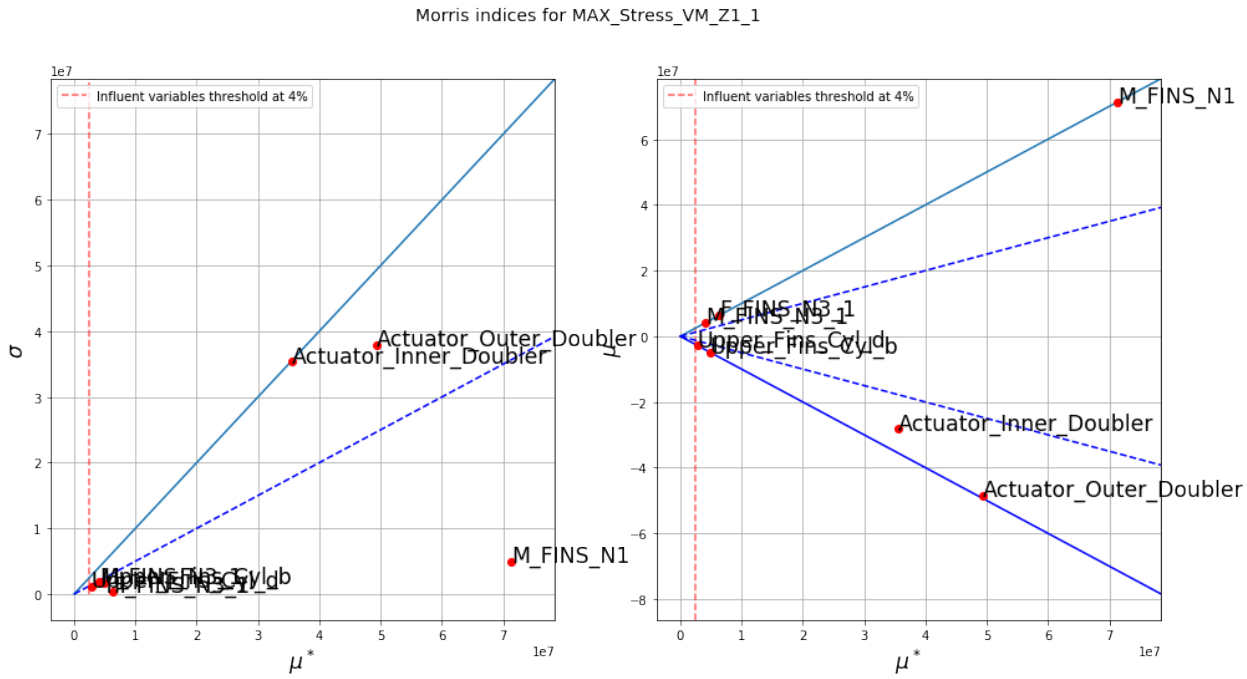


Figure 7: Morris graphics for the first Von Mises stress output.

### 3.2.2 Sensitivity analysis

The Sobol indices are computed using the Polynomial Chaos Expansion (PCE) surrogate model. In order to build this metamodel a design of experiments (optimized Latin Hypercube) of size 850 has been computed. In order to validate the metamodel, the leave-one-out cross validation criterion $Q^2$ is computed as well as a $R^2$ using a test sample of 720 points, also built with an optimized Latin Hypercube DOE. All these validation values are greater than 0.92 for the three outputs so the metamodel can be used with confidence in further analysis.

N.B. : in order to get an accurate PCE, for each output, only its own influential input variables were considered.

From the PCE, Sobol indices are computed for the 3 outputs. Results are shown in Figure 8, the main influential variable for the 3 outputs is the force $M\_FINS\_N1$ with a first order indices value at least 0.5. The first order and total order indices are almost equal, which means that no interaction of some inputs has influence on the output variability.

It also shows that the selected thicknesses have different influences according to the chosen output. The input *Actuator_Outer_Doubler* is important for the first VM stress and the flux whereas it is not for the second VM. *Actuator_Inner_Doubler* is only influential for the first VM, and $Upper\_Fins\_Cyl\_b$ $Upper\_Fins\_Cyl\_d$ are important for the second VM. To finish the last forces ($F\_FINS\_N3\_1$ and $M\_FINS\_N3\_1$) may not be considered as influential, they were selected during the screening analysis (it only uses bounds) but taking into account their input distribution in Sobol' analysis reduces their influence to almost nothing.

### 3.2.3 Probability evaluation

The current problem needs to take into account 3 failure events, each associated to one outputs. The probability of failure that must be computed is defined in Equation 26. This is a union event of the 3 individual events.

DOI: 10.13009/EUCASS2022-6153



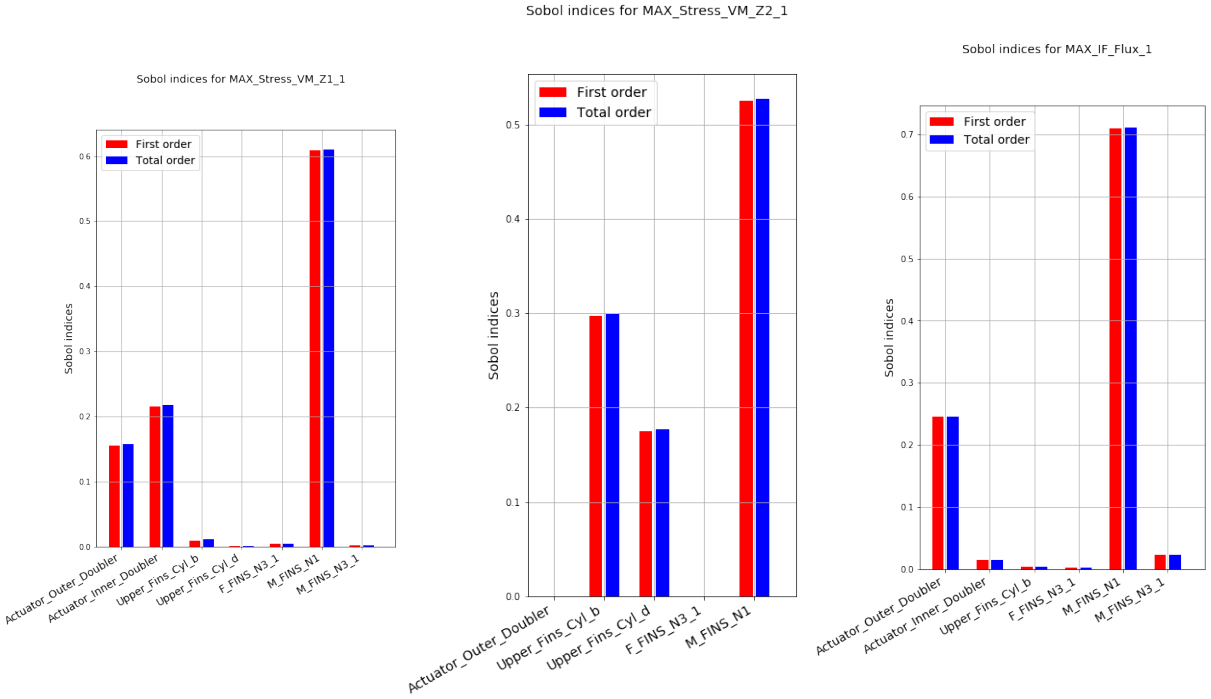


Figure 8: Sobol indices of the 3 outputs (2 Von Mises stress and one flux).

$$\begin{aligned} P_f &= \text{Prob}(MAX\_Stress\_VM\_Z1 > 4.2 \times 10^8) \\ &\quad \cup \text{Prob}(MAX\_Stress\_VM\_Z2 > 4.56 \times 10^8) \\ &\quad \cup \text{Prob}(MAX\_IF\_Flux > 8.3 \times 10^5) \\ &= \text{Prob}(E_1 \cup E_2 \cup E_3) \end{aligned} \tag{25}$$

Here the events $E_1$, $E_2$ and $E_3$ are introduced to simplify the notation in the optimization section.

This probability can be estimated using several reliability technique : Monte Carlo simulation, FORM + Importance Sampling, Subset simulation or metamodel-based technique. In the current study, due to a lack of time, the PCE metamodel built for the Sobol' analysis has been used to compute the probability of failure. In order to avoid to do prediction outside the domain of definition, the design of experiments used to build the metamodel was built from an extended distribution. The coefficient of variation of the input random variables were 4 times greater than the original definition.

Results of the probability failure are given in table 1. The three estimation techniques provides equivalent results.

Table 1: Probability of failure result values

| Method | Probability value | 95% confidence length |
|---|---|---|
| Monte Carlo simulation | $6.38 \times 10^{-3}$ | $1.25 \times 10^{-3}$ |
| FORM System | $5.70 \times 10^{-3}$ | None |
| Importance sampling | $6.54 \times 10^{-3}$ | $1.28 \times 10^{-3}$ |

Importance factors can be derived from the simulations, it corresponds with a reliability sensitivity. This is the weight of each inputs regarding the failure of the system. These factors are shown in Figure 9, it can be seen that the force $M\_FINS\_N1$ is the most important, which is consistent with the Sobol indices. Secondly the thickness *Actuator_Outer_Doubler* appears also as an important variable.

### 3.2.4 RBDO

The optimization performed consist in minimizing the sum of the thickness variables, with the constraint that the probability of failure remains lower than a probability threshold. The current used optimization algorithm does not

DOI: 10.13009/EUCASS2022-6153



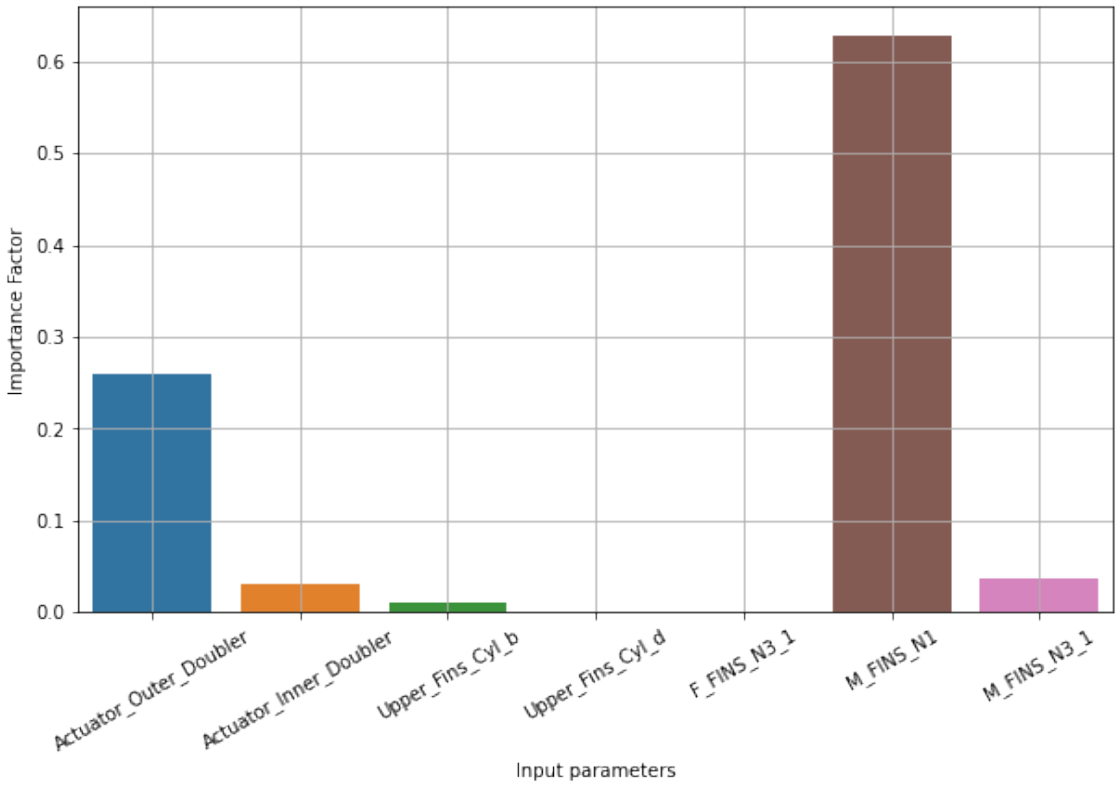


Figure 9: Reliability importance factors.

allow to optimize the random variables, only deterministic parameters can be optimized. So all thicknesses will be now considered as deterministic parameters. However to keep a conservative estimation of the probability of failure, the chosen constant value will not be the mean but the quantile at 1% of the original distribution (Gaussian with 3% of coefficient of variation)

Let be $\mathcal{P}$ the set of the optimization variables
$\mathcal{P} = \{Actuator\_Outer\_Doubler, Actuator\_Inner\_Doubler, Upper\_Fins\_Cyl\_b, Upper\_Fins\_Cyl\_d\}$ and $\mathcal{X}$ the set of the random variables $\mathcal{X} = \{F\_FINS\_N3\_1, M\_FINS\_N1, M\_FINS\_N3\_1\}$.

The optimization problems writes :

$$min_{\mathcal{P}} \quad \sum_{p \in \mathcal{P}} p \tag{26}$$

$$s.t. \quad \text{Prob}(E_1 \cup E_2 \cup E_3) < P_{f,threshold} \tag{27}$$

$$\mathcal{P}_{min} \leq \mathcal{P} \leq \mathcal{P}_{max} \tag{28}$$

with $\mathcal{P}_{min}$ and $\mathcal{P}_{max}$ are the boundaries of the optimized parameters.

This optimization problem has been solved using a global optimization algorithm from the NLopt library (Steven G. Johnson, http://github.com/stevengj/nlopt), named *GN_ORIG_DIRECT_L* [10]. The probability threshold is set to $P_{f,threshold} = 10^{-3}$.

The table 2 sums up the main value of the optimization results. It shows that the objective has been slightly minimized (loss of $6 \times 10^{-4}$). However in the same time the probability of failure has been improved, as it respects the given threshold. This means that some critical thicknesses have been increased in order to improve the reliability and in the same time less important thicknesses decreased making the total thickness lower than at the initial start.

Eventually it is possible to update the probability of failure computed in the section 3.2.3 by considering once again the thicknesses as random variables. First it requires to compute the mean of these thicknesses assuming the optimized values are the quantiles at 1% of Gaussian distribution with 3% of coefficient of variation.

The probability of failures before and after the optimization procedure are given in table 3.

DOI: 10.13009/EUCASS2022-6153



Table 2: Optimization under uncertainty results

| | |
|---|---|
| Initial objective (at the quantile values) | 0.0474 |
| Initial probability of failure | $3.4 \times 10^{-3}$ |
| Final objective (at the quantile values) | 0.0468 |
| Final probability of failure | $9.9 \times 10^{-4}$ |

Table 3: Probability of failure after the optimization steps

| Thickness mean | Probability estimation (importance sampling) | 95% confidence length |
|---|---|---|
| Original mean | $6.54 \times 10^{-3}$ | $1.25 \times 10^{-3}$ |
| Modified mean | $3.73 \times 10^{-5}$ | $7.30 \times 10^{-6}$ |

## 4. Conclusion

This paper presents a reliability-based design optimization (RBDO) of a part of a launcher using a mechano-probabilistic optimization module, which is developed by Phimeca based on the OpenTURNS library. The objective is to apply the probabilistic methods to the field of launchers by optimizing the design of the vehicle equipment bay and considering the inherent uncertainties of the system.

A screening analysis is first performed in order to reduce the number of uncertain inputs. The analysis shows that among the 47 random inputs, only three of them are to be considered in the probabilistic design. Then, for the failure probability estimation, three failure events were considered, each one of them is associated to one output. The problem is treated as a problem system and three reliability methods are used: Monte Carlo simulation, FORM system and importance sampling. The results of the three methods converge roughly to the same estimate for the failure probability.

The final step of this study is the RBDO. The aim is the reduce the sum of the thickness variables under the constraint that the failure probability should not exceed a given threshold. In the present study, it is shown that the critical thicknesses have to be increased, unlike the less important ones which can be reduced. Thus, the reliability is improved and the total thickness decreased compared to the initial one.

## References

[1] T Abdo and R Rackwitz. A new beta-point algorithm for large time-invariant and time-variant reliability problems. In *Reliability and Optimization of Structural Systems 90*, pages 1–12. Springer, 1991.

[2] Younes Aoues and Alaa Chateauneuf. Benchmark study of numerical methods for reliability-based design optimization. *Structural and multidisciplinary optimization*, 41(2):277–294, 2010.

[3] Siu-Kui Au, Costas Papadimitriou, and James L Beck. Reliability of uncertain dynamical systems with multiple design points. *Structural Safety*, 21(2):113–133, 1999.

[4] Michaël Baudin, Anne Dutfoy, Bertrand Iooss, and Anne-Laure Popelin. *OpenTURNS: An Industrial Software for Uncertainty Quantification in Simulation*, pages 1–38. Springer International Publishing, Cham, 2016.

[5] Hans-Georg Beyer and Bernhard Sendhoff. Robust optimization–a comprehensive survey. *Computer methods in applied mechanics and engineering*, 196(33-34):3190–3218, 2007.

[6] Oussama Braydi, Pascal Lafon, and Rafic Younes. On the formulation of optimization problems under uncertainty in mechanical design. *International Journal on Interactive Design and Manufacturing (IJIDeM)*, 13(1):75–87, 2019.

[7] F. Campolongo, S. Tarantola, and A. Saltelli. Tackling quantitatively large dimensionality problems. *Computer Physics Communications*, 117(1):75–85, 1999.

[8] Ove Ditlevsen and Henrik O Madsen. *Structural reliability methods*, volume 178. Wiley New York, 1996.

[9] I Enevoldsen and John Dalsgaard Sørensen. Reliability-based optimization in structural engineering. *Structural safety*, 15(3):169–196, 1994.

DOI: 10.13009/EUCASS2022-6153



[10] J.M. Gablonsky and C.T. Kelley. A Locally-Biased form of the DIRECT Algorithm. *Journal of Global Optimization*, 21(1):27–37, 2001.

[11] A Harbitz. Efficient and accurate probability of failure calculation by the use of importance sampling technique. In *Proc. of ICASP*, volume 4, pages 825–836, 1983.

[12] Michael Hohenbichler and Ruediger Rackwitz. First-order concepts in system reliability. *Structural safety*, 1(3):177–188, 1982.

[13] Laure Jaeger. *Optimisation multidisciplinaire sous incertitude en phase conceptuelle avion*. PhD thesis, Toulouse 3, 2013.

[14] Hector A Jensen, Marcos A Valdebenito, Gerhart I Schuëller, and Danilo S Kusanovic. Reliability-based optimization of stochastic systems using line search. *Computer methods in applied mechanics and engineering*, 198(49-52):3915–3924, 2009.

[15] Nicolas Lelièvre, Pierre Beaurepaire, Cécile Mattrand, Nicolas Gayton, and Abdelkader Otsmane. On the consideration of uncertainty in design: optimization-reliability-robustness. *Structural and Multidisciplinary Optimization*, 54(6):1423–1437, 2016.

[16] Maurice Lemaire, Alaa Chateauneuf, and Jean-Claude Mitteau. *Structural reliability*. Wiley Online Library, 2009.

[17] Robert E Melchers and André T Beck. *Structural reliability analysis and prediction*. John wiley & sons, 2018.

[18] Max D. Morris. Factorial Sampling Plans for Preliminary Computational Experiments. *Technometrics*, 33(2):161, May 1991.

[19] Andre Nataf. Determination des distribution dont les marges sont donnÃ©es. *Comptes Rendus de l Academie des Sciences*, 225:42–43, 1962.

[20] Rüdiger Rackwitz and Bernd Flessler. Structural reliability under combined random load sequences. *Computers & structures*, 9(5):489–494, 1978.

[21] Murray Rosenblatt. Remarks on a multivariate transformation. *The annals of mathematical statistics*, 23(3):470–472, 1952.

[22] Masanobu Shinozuka. Basic analysis of structural safety. *Journal of Structural Engineering*, 109(3):721–740, 1983.

[23] I.M Sobol'. Global sensitivity indices for nonlinear mathematical models and their Monte Carlo estimates. *Mathematics and Computers in Simulation*, 55(1-3):271–280, February 2001.

[24] Erik H Vanmarcke. Matrix formulation of reliability analysis and reliability-based design. *Computers & Structures*, 3(4):757–770, 1973.

[25] Wen Yao, Xiaoqian Chen, Wencai Luo, Michel Van Tooren, and Jian Guo. Review of uncertainty-based multidisciplinary design optimization methods for aerospace vehicles. *Progress in Aerospace Sciences*, 47(6):450–479, 2011.